Research Journal of Applied Sciences 2 (4): 505-511, 2007

Variability of Column-Integrated Aerosol Turbidity and Radiative Parameters in Sub-Saharan West Africa

K.O. Ogunjobi
Department of Meteorology, Federal University of Technology, Akure, Nigeria

Abstract: Spectral aerosol turbidity measurements over Ilorin, Nigeria acquired through ground-based Sun-sky radiometer from 340-1020nm are analyzed from April 1998-April 2006. Aerosols Optical Thickness (AOT) obtained showed a pronounced temporal trend, with maximum aerosol loading during the December-March period. Interannual variations in daily and monthly mean Angstrom exponent (α) were also observed, resulting from differences in the bimodal aerosol size distributions. Aerosol size distribution retrievals obtained from combined solar extinction and sky irradiance measurements were also utilized in the analysis. Result shows that the fine mode particle exhibits relative stability throughout the different seasons, while the coarse fraction changes significantly. The aerosol size distributions for the December-March period yields two modes of large or coarse particles with radius near 1.71 and 3.86 μm (for December and February) or 5.06 (for January and March). Further analysis shows large differences in the asymmetric factor during 1999, 2001 and 2005 in high (Infrared) wavelengths, but relatively little changes in the short (Visible) wavelengths during the dry months of December to March.

Key words: Aerosol optical thickness, size distribution, Angstrom exponent, asymmetric factor

INTRODUCTION

Tropospheric aerosols influence the earth's climate in divers ways however not all of them are well known. The direct cooling effect of aerosols on climate, by scattering a fraction of the incoming solar radiation back to space, is well understood. The radiative heating effect produced by aerosol absorption of short and longwave radiation has been found to produce changes in net heating rates (Alpert *et al*., 1998). In addition, aerosols can indirectly affect climate through their action as cloud condensation nuclei (Charlson *et al*., 1992; IPCC, 2001). The evaluation of aerosol radiative forcing effect on climate (the net radiation flux change at the top of the atmosphere due solely to the effect of atmospheric aerosols), requires global data on aerosol properties and amounts over both the oceans and the continents. Aerosol effects are also significant in non-climate related processes, such as those related to the analysis of local, regional and global air pollution. Large-scale biomass burning and boreal forest fire events often cast huge smoke plumes thousands of kilometers away from their sources, causing serious air quality and health related problems (Gupta *et al*., 2006).

Saharan dust optical properties are important for various estimations of radiative forcing inasmuch as dust plays an important role in radiative processes. Knowledge of aerosol characteristics on a global scale, their temporal change and interrelations with other atmospheric parameters is of great importance in understanding the mechanisms which define the aerosol optical state of the atmosphere. Optical aerosol climatology is a supplementary means for extracting information required in atmospheric correction methods (d'Almeida *et al*., 1987). The validation of aerosol optical properties derived from satellite data also requires investigations of atmospheric aerosol optical state (Kaufman and Tanre, 1994).

The Sahara desert region is one of the most extensive sources of mineral dust in the northern hemisphere (Husar *et al*., 1997). Mineral dust, being considered as part of natural background aerosol is suggested to be an important climate-forcing component over specific oceanic areas and other regions where dust concentrations are high (Li *et al*., I996).

This study investigates the atmospheric aerosol optical properties over a sub-Saharan West Africa station; seasonal variability of aerosol optical thickness and its spectral behaviour. The AERONET solar attenuation and sky brightness measurements are used to derive the spectral optical thickness and size distribution of the column ambient aerosol. In contrast to in situ measurements, AERONET remote measurements do not characterize the aerosol chemical composition, but measure the optical properties of the aerosol, unaffected by sampling and drying processes inherent in situ methods (Smirnov *et al*., 2000).

MEASUREMENT STRATEGY

The measurements presented in this paper were data collected at Ilorin from the Aerosol Robotic Network (AERONET) automatic Sun/sky radiometers. The site is located on the campus of the university of Ilorin, Nigeria (08 19N, 04 20 E, 350 m asl), at the upper tip of the Guinea savannah zone in sub-Sahel Nigeria. The instrument deployed in the network is an automatic CIMEL Elctronique CE-318 Sun-Sky radiometer. The CIMEL radiometers are described in detail by Holben *et al.* (1998) however, a brief description will be given here. The automatic tracking Sun and sky scanning radiometers made direct Sun measurements with a 1.2 degree full field of view every 15 min at 340, 380, 440, 500, 670, 870, 940 and 1020 nm. The direct Sum measurements take ~8s to scan all the 8 wavelengths . The measured solar extinction are then used to compute aerosol optical depth at each wavelength except for the 940 nm channel, which is used to retrieve total column water vapour in cm (Bruegge *et al.*, 1992).

The Angstrom exponent α, defined by the wavelength dependence of the optical thickness is determined as

$$\alpha = -\frac{\ln(\tau_{1020nm}/\tau_{500nm})}{\ln(1020/500)}$$

where τ is the optical thickness for the 1020 and 500nm wavelength bands. This parameter is used as a rough measure of the aerosol type, in which large dust particles are dominant for α <0.5 and those in which small pollution or smoke particles are dominant for α>1.0 (Kaufman *et al.*, 2000). It is suggested that between these two thresholds, the aerosol is a mix of the two modes.

Calibration of the field instruments was performed by the transfer of calibration from a reference instrument which has been calibrated by the Langley plot technique at Mauna Loa Observatory (MLO), Hawaii. Reference instruments are typically calibrated at MLO every 2-3 months using morning measurements only. The combined effects of uncertainties in calibration, atmospheric pressure and total ozone amount result in a total uncertainty of ~0.010-0.021 in computed aerosol optical thickness.

The CIMEL sky radiance almucantar measurements at 440, 670,870 and 1020 nm in conjunction with the direct Sun measured AOT at these wavelengths were used to retrieve aerosol size distributions following the method of Dubovik and King (2000). Almucanter sky radiance measurements were made at optical air masses of 4, 3 and 2 in the morning and afternoon and once per hour in between.

RESULTS

Figure 1 shows the monthly average aerosol optical thickness estimated at different wavelengths and the precipatable water vapour for measurements made from April 1998-April 2006. The standard error of the mean AOT represented by the vertical bar over each month is a measure of the scatter of individual optical depths that have been used to obtain the monthly averages. The data have been screened for clouds, following the methodology of Smirnov *et al.* (2000). This technique relies on the greater temporal variance of cloud optical depth against the AOT therefore temporal and spatially uniform cloud may at times be misidentified as cloud-free (Eck *et al.*, 2003). Multiyear averages are necessary in order to characterize a truly representative climatologically seasonal cycle. The plot shows significant month-to-month variation in AOT and its dependence on wavelength. The monthly mean AOT at all wavelengths show maximum value during the d ry season (December-March) and minimum during wet season (May-September). The seasonal peak during the dry season may be attributed to the prevailing northeasterly winds otherwise known as the Harmattan from long range transport of Saharan aerosol dust from the Chad basin to Nigeria (Westphal *et al.*, 1988; Pinker *et al.*, 2001). It is also interesting to note the decrease in AOT from April to October which may be attributed to the dust-free clean air condition by cloud scavenging and wet removal processes during the summer and early fall at Ilorin. Also evident from Fig. 1 is the decrease in AOT values as wavelength increases. Similar variability has been reported by Holben *et al.* (1991), Ogunjobi *et al.* (2003). The annual average aerosol optical thickness for the whole period of observations decreases from 0.74±0.37 to 0.41±0.23 at 340–1020nm wavelengths. As expected, the precipitable water vapour, pwv (cm) is maximum during summer months (Fig. 1), that corresponds to the northern most position of the ITCZ (May-September) and minimum in the dry season (November -March). The pwv increased from an average of 2.50±0.33 cm during the dry winter months to values greater than 4.50cm in May through September.

Extreme large day-to-day variability in daily mean of AOT and α at Ilorin was observed during the harmattan dust seasons (Fig. 2a-b). Large day-to-day variation of this magnitude may be driven by a combination of many meteorological factors including air parcel trajectory, temperature inversions and dust storms associated with high winds. Daily means of AOT spread from 0.09 to 0.6 for most of the cases except for the months of June to

August where daily optical thickness fluctuations are less pronounced varying around 0.25. The derived monthly averaged aerosol optical thickness at λ = 500nm and the Angstrom exponent ($\alpha_{380\text{-}500nm}$) also computed for 380 and 500nm is shown in Fig. 3a-b. The computed data are consistent in showing that monthly AOT values generally vary between 0.3 and 1.0. Highest AOT values are obtained in January-February and lowest values generally in July-September (Fig. 3a). The uncertainty bars are one standard deviation around the mean overall studied period. The highest uncertainty in the retrieved AOT was observed during the January – March period which may be attributed to the influx of dust transport from different source region during the harmattan dust spell. The higher and lower values of $\alpha_{380\text{-}500nm}$ correspond to the lower and higher values of AOT.

Angstrom exponent is observed to increase rapidly to a secondary peak during the May-August period when AOT decrease to its lowest monthly values due to scavenging of the atmosphere by precipitation. The high Angstrom exponent observed in December through March period (Fig. 3b) may be attributed to the mixing of

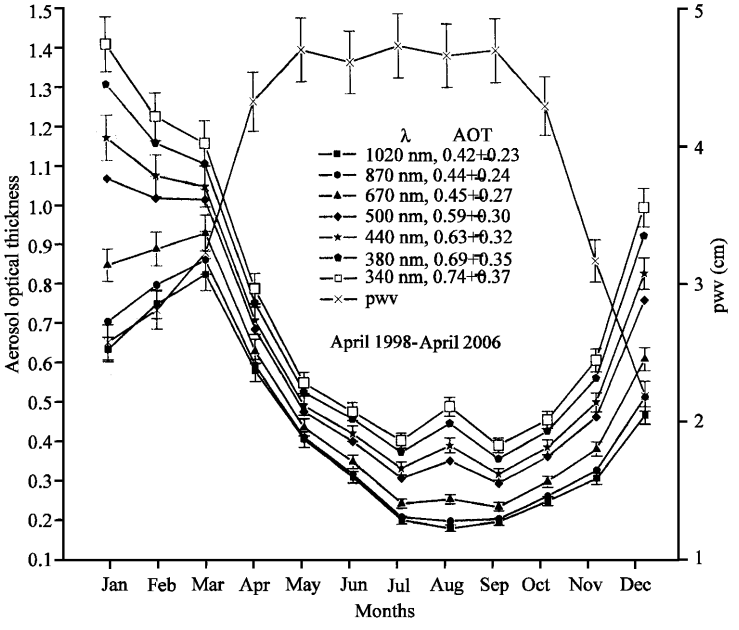

Fig. 1: Spectral monthly mean of aerosol optical thickness at Ilorin, from April 1998-April 2006. Also shown are the error bars which indicate the±1 standard deviation

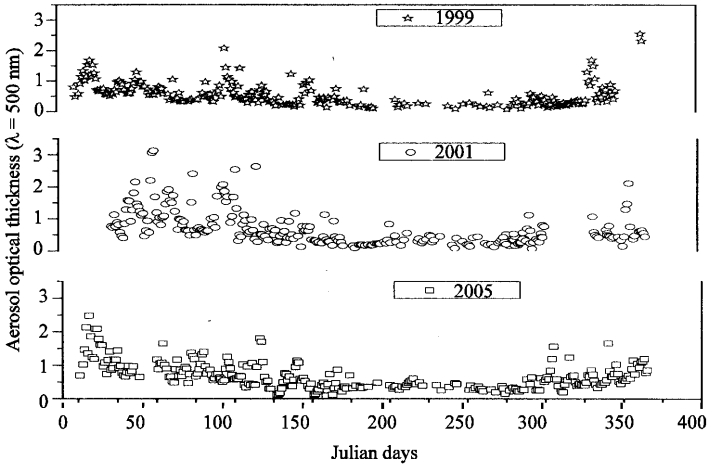

Fig. 2a: Time series of the daily average values of AOT for cloud free days during January to December 1999, 2001 and 2005 at Ilorin, depicting large day-day-variability

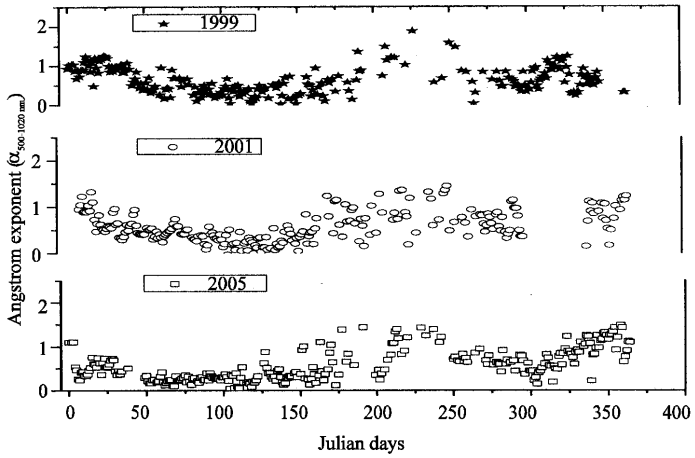

Fig. 2b: Same as in Fig 2a, but measurements are for daily mean α values estimated for two wavelengths 500 -1020nm

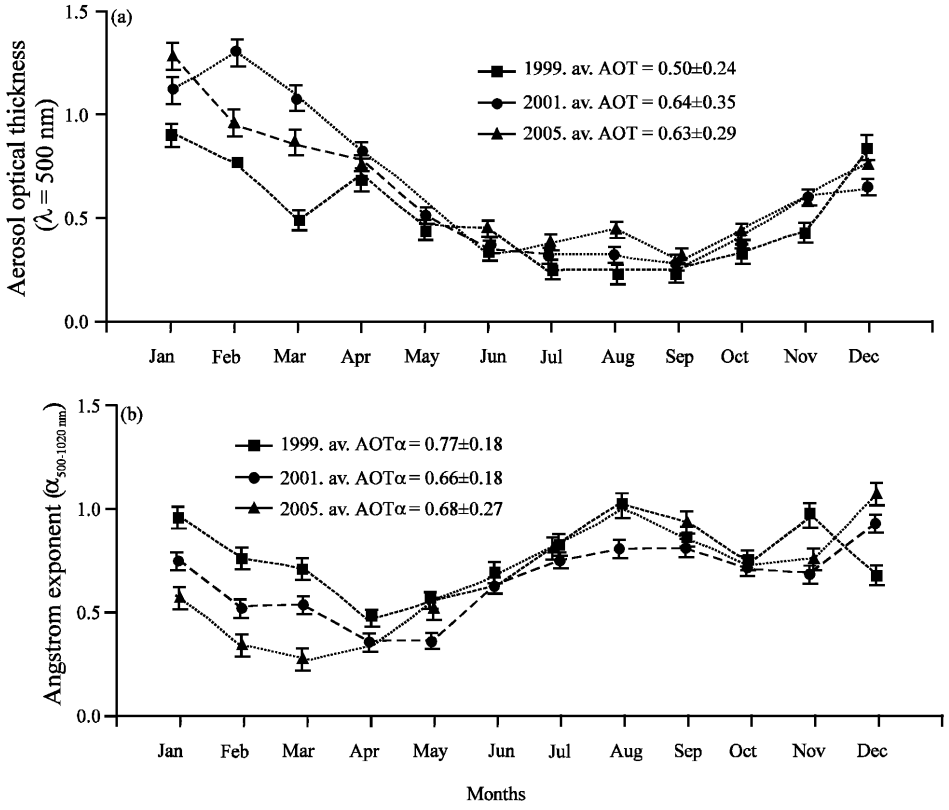

Fig. 3: Monthly average aerosol optical thickness at the 500-nm wavelength and Angstrom exponent. Error bars show one standard deviation of the daily average values

prevalent dust particle with biomass burning which is a common practice at Ilorin during the harmattan dry seasons. The largest values of AOT are associated with small values of α which is characteristic of the presence of dust while small AOT values are associated with large α values. This trend is similar to result of desert dust aerosol optical depth and Angstrom exponent reported by Holben *et al*. (2001) at Banizoumbou, Niger. During the period of measurements, the turbidity is always significantly above background levels during the dry seasons. Analysis shows that from January through March, the very low Angstrom exponent confirms the presence of dust in 2005 (Fig. 3b). In December and January during 1999 and 2001, there is evidently a second aerosol type that contributes to the turbidity as confirmed by the higher values of Angstrom exponent. At that time,

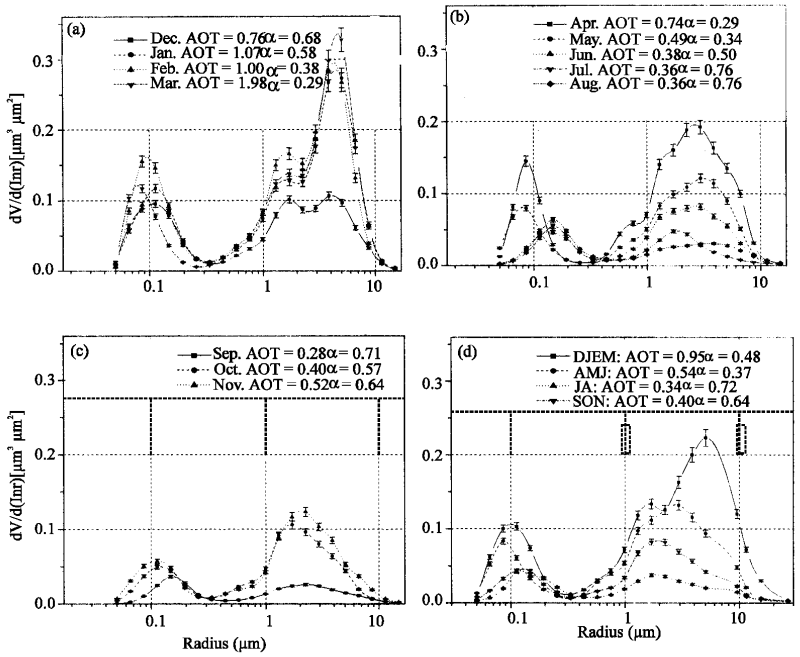

Fig. 4: Seasonal aerosol volume distribution in the total atmospheric column at Ilorin. The retrievals were derived as the monthly average aerosol size distributions from simultaneous analyses of sky radiances in the almucantar and spectral AOT at 440, 670, 870 and 1020nm

aerosols resulting from biomass burning activities are then mixed with dust depending on the wind direction.

Figure 4a-d illustrate seasonal and monthly averaged aerosol size distribution (dV/dlnR). Also shown are the aerosol optical thickness (λ=500nm) and the computed Angstrom exponent for 380 -500nm. It should be noted that we have assigned particles with radius 0.05< r < 0.3-0.6 and 0.3-0.6< r < 15 as fine and coarse modes particles, respectively. The dominant variations in these plot can be directly associated with the distinct changes in the amplitude and spectral dependence of the aerosol optical thickness data. The fine mode particle shows relative stability, while the coarse fraction changes significantly.

Result in Fig. 4a shows that the aerosol size distribution for December-March (winter dust spell seasons) yields two modes of large or coarse particles with radius near 1.71 μm and 3.86 μm during December and February or 5.06 μm for the months of January and March. The variation in the magnitude and shape of the coarse aerosol fraction between December-March can be explained by the incoming dust during the winter dust seasons. Figure 4b shows that the fine mode particle radius is nearly stable at 0.086μm for all months of the year except May-July that exhibits a slight shift to a higher radius of 0.15μm in the fine mode region. Figure 4c also shows a reduction in the aerosol volume size distribution during the September- November period. Also evident is the reduction in the aerosol optical thickness of the coarse mode dust particle. For example the coarse mode volume distribution in September is observed to reduce to nearly a third of the retrieved values for March when monthly average AOT reduces from 0.98 ($\alpha_{380\text{-}500nm}$= 0.29) to as low as 0.28 ($\alpha_{380\text{-}500nm}$= 0.71). Figure 4d shows that there is a great possibility for increasing particle size as aerosol optical depth increases, for example, the peak in the distribution of the coarse mode volume radius of the aerosol at Ilorin increases from ~1.71 μm during the monsoon month of August (AOT = 0.34, $\alpha_{380\text{-}500nm}$= 0.71) to ~5.06 μm during dust storm periods of December-March (AOT= 0.95, $\alpha_{380\text{-}500nm}$= 0.48).

The scattering phase function for the aerosols was obtained from Mie calculations utilizing the retrieved volume size distributions and the refractive indices from the sky radiances and the spectral aerosol optical thickness data. The retrieved phase function values were in turn used to compute the asymmetric factor *g*, which is the average cosine of the scattering direction weighted by the phase function. The asymmetric factor equals 1 for pure forward scattering and -1 for completer backscattering (Eck *et al*., 2001). A comparison of the spectral asymmetric parameter between the years 1999, 2001 and 2005 during period of high turbidity (December to March) and periods of low optical thickness (May-September) is presented in Fig. 5. Asymmetric factor *g* is observed to decrease with increase in wavelength for all

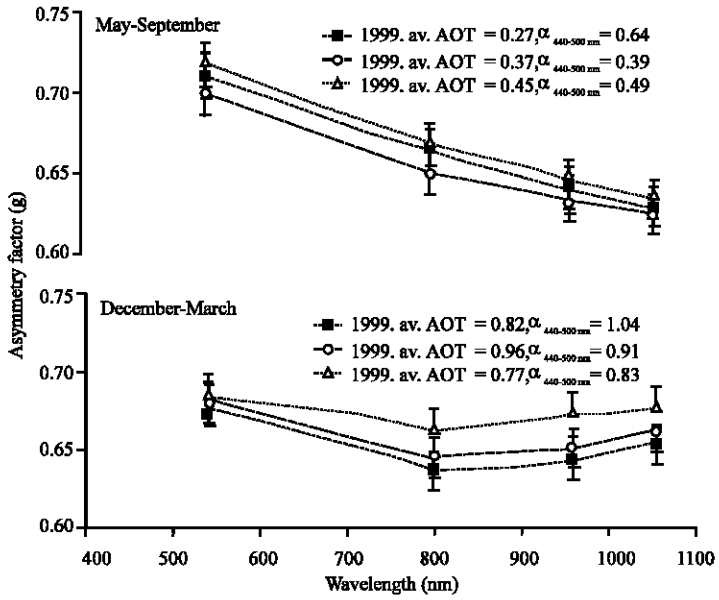

Fig. 5: Spectral asymmetric factor (g) at Ilorin from May-September and those from December to March. Also shown are the computed average AOT, Angstrom exponent and the error bars show one standard deviation of the individual retrievals

years during May-September period while it increases at higher wavelengths (870-1020nm) during the December-March period. The greater relative contribution of coarse mode particles during the winter months (December-March) to the aerosol size distribution resulted in a phase function shift toward greater forward scattering at the longer (infrared) wavelengths while there is no significant contribution during the May-September period largely due to dust-free atmosphere.

CONCLUSION

Measurements of spectral aerosol optical thickness and directional sky radiances were made with AERONET Sun-sky radiometers in a sub-Saharan Africa site from April 1998-April 2006 to characterize the aerosol optical properties and their interannual variability. The principal findings are summarized as follows:

- Large interannaul variability of aerosol optical thickness was observed at Ilorin during the harmattan dust episode of December through March. For example the monthly averages of AOT (λ=500nm) in February and March 2001 were approximately 70 and 118% as high values estimated for 1999, with the year 2005 being intermediate in magnitude.
- Spectral variations of AOT as parameterized by the Angstrom exponent α also exhibits interannual variability, with lower monthly averages values of α values in 2005 and higher values in 1999 during the January-March period. This is the result of relative greater contribution of coarse-mode particles to the total optical thickness in 2005 than in 1999. Seasonal variations of the optical parameters showed that the dust aerosol concentrations were a major contributor to optical thickness and Angstrom exponent variability at Ilorin.
- Optical inversion of sky radiance and optical thickness data indicate that the variations in aerosol volume size distributions over Ilorin were largely due to changes in the concentrations of the coarse aerosol fractions. The asymmetric factor (g) which is primarily governed by the size distribution also showed interannual variations for 1999, 2001 and 2005. The magnitude of g increases during the December-March period in the infrared wavelengths (870-1020 nm), but decreased sharply for all years in the visible wavelength (440-670 nm).

ACKNOWLEDGMENT

We acknowledge the critical roles of the Principal Investigator (Prof R.T Pinker) and the site managers (Dr. Clement Akoshile and Prof T.O Aro) for their effort in establishing and maintaining long-term observations at the Ilorin AERONET site. The author wishes to also acknowledge the support of Alexander von Humboldt Foundation.

REFERENCES

Alpert, P., Y.J. Kaufman, Y. Shay-el, D. Tanre, A. Da Silva and Y.H. Joseph, 1998. Dust forcing of climate inferred from correlations between dust data and model errors. Nature, 395: 367-370.

Bruegge, C.T., J.E. Conel, R.O.Green, J.S. Margolis, R.G. Holm and G. Toon, 1992. Water vapour column abundance retrievals during FIFE, J Geophys. Res., 97: 18759-18768.

Charlson, R.J., S.E. Schwartz, J.M. Hales, R.D. Cess, J.A. Coakley Jr., J.E. Hansen and D.J. Hofmann, 1992. Climate forcing by anthropogenic aerosols. Science, 255: 423-430.

d'Almeida, G.A., 1987. On the variability of desert aerosol radiative characteristics. J. Geophys. Res., 92: 3017-3026.

Dubovik, O. and M.D. King, 2000. A flexible inversion algorithm for retrieval of aerosol optical properties from Sun and sky radiance measurements. J. Geophys. Res., 105: 673-20,696.

Eck, T.F. *et al*., 2003. Variability of biomass burning aerosol optical characteristics in southern Africa during the SAFARI 2000 dry season campaign and a comparison of single scattering albedo estimates from radiometric measurements, J. Geophys. Res., 108, 8477, doi: 10.1029/2002JD002321.

Eck, T.F. *et al*., 2001. Column-integrated aerosol optical properties over the Maldives during the northeast monsoon for 1998-2000. J. Geophys. Res., 106: 28555-28566.

Gupta, P., S.A. Christopher, J. Wang, R. Gehrig, Y.C. Lee and N. Kumar, 2006. Satellite remote sensing of particulate matter and air quality over global cities, Atmospheric Environment, 40: 5880-5892.

Holben, B.N. *et al*., 2001. An emerging ground-based aerosol climatology: Aerosol optical depth from AERONET. J Geophys. Res., 106: 12067-12097.

Holben, B.N. *et al*., 1998. AERONET-A federated instrumentation network and data archive for aerosol characterization. Remote Sens. Environ., 66: 1-16.

Holben, B.N., T.F. Eck and R.S. Fraser, 1991. Temporal and spatial variability of aerosol optical depth in the Sahel region in relation to vegetation remote sensing. Int. J. Rem. Sens., 12: 1147-1163.

Husar, R.B., J.M. Prospero and L.L. Stowe, 1997. Characterization of tropospheric aerosols over the oceans with the NOAA advanced very high resolution radiometer optical thickness operational product, J. Geophys. Res., 102: 16,889-16,909.

Intergovernmental Panel on Climate Change (IPCC), 2001. Climate Change the Scientific Basis (Eds.), J.T. Houghton *et al*., Cambridge University Press New York, pp: 881.

Kaufman, Y.J. *et al*., 2000. Detection of dust over the desert by EOS-MODIS, IEEE. Trans. Geos. Remote Sens., 38: 525-531.

Kaufman, Y.J. and D. Tanre, 1994. Effect of variations in supersaturation on the formation of cloud condensation nuclei. Nature, 369: 45-48.

Li, X., H. Maring, D. Savoie, K. Voss and J.M. Prospero, 1996. Dominance of mineral dust in aerosol light-scattering in the North Atlantic trade winds, Nature, 380: 416-419.

Ogunjobi, K.O., Y.J. Kim and Z. He, 2003. Aerosol optical properties during Asian dust storm episodes in South Korea, Theor. Applied Climatol., 76: 65-75.

Pinker, R.T., G. Pandithurai, B.N. Holben, O. Dubovik, T.O. Aro, 2001. A dust outbreak episode in Sub-Sahel West Africa. J. Geophys. Res., 106: 22923-22930.

Smirnov, A., B.N. Holben, T.F. Eck, O. Dubovik and I. Slutsker, 2000. Cloud screening and quality control algorithms for the AERONET database, Rem. Sens. Environ., 73: 337-349.

Westphal, D.L., O.B.Toon and T.N. Carlson, 1988. A Case Study of Mobilization and Transport of Saharan Dust. J. Atmos. Sci., 45: 2145-2175.